

# HYPersonic MISSILES – SOME AEROTHERMODYNAMIC PROBLEM AREAS

R A East, University of Southampton, UK  
J A Edwards, DERA, UK

**Keywords:** *hypersonic, kinetic heating, interference effects, aerothermodynamics*

## Abstract

*Hypersonic weapon systems encounter a number of potential kinetic heating problems. In particular, interference effects associated with the presence of aerodynamic devices to aid stability and control can lead to significant local increases in heat transfer rate. This paper reviews the interference effects associated with flare and fin stabilisers and with the use of control jets. It is shown that many of these flows are extremely complex and present significant computational challenges. Emphasis is given to reviewing the physics of these flows as revealed by experiments.*

## 1 Introduction

Over the last ten to fifteen years the thrust for hypersonic systems for military applications has changed from emphasis on aero-space planes for the delivery of rapid reaction force over long ranges to relatively short range response to time critical targets (e.g. mobile missile launchers, ABM defence, TMD, etc.). In addition, with increasing sophistication of ground and air launched defence systems, increasing the speed of attack weapons has attractions in limiting enemy response capability. While the need for hypersonic studies for systems engaged in exo-atmospheric engagements has not changed, since the requirement to reach orbital velocities introduces the traditional hypersonic problems associated with rocket launchers, manoeuvre within the upper or lower atmosphere introduces a new set of problems and constraints. As well as ground and air launched missile systems, there has been renewed emphasis on research into gun launched hypersonic kinetic energy projectiles for defeat of new armour concepts

and other hardened ground targets. Within the United Kingdom, kinetic energy anti-tank projectiles have been launched at speeds approaching 2.4 km/sec using conventional propellants, and in the US at speeds of 2.8 km/sec from electromagnetic guns (rail guns).

Over the next twenty years, or so, propulsion systems for tactical hypersonic missiles are likely to continue to be based on solid fuel rockets. The possible development of long range, high speed, air launched, precision strike missiles may provide a notable exception to this view, since air-breathing propulsion could have significant advantages. In this case, the development of supersonic combustion ramjets (scramjets) with hydrocarbon fuel could provide propulsion systems capable of speeds up to Mach 8. Such systems are likely to have integrated engine-airframe geometries along the lines of the later United States NASP concepts. However, discussion of propulsion systems and engine-airframe integration lies outside of the scope of this paper. We therefore limit our arguments to missiles with, at most, small deviations from conventional shapes.

While pure speed has the advantages alluded to in the above paragraph, for tactical systems engaging aircraft or missiles it has a significant disadvantage. In manoeuvre, a vehicle undertaking a constant radius turn has to “pull” a greater lateral acceleration as the speed increases. This has significant impact on the required aerodynamic control authority for certain mission specifications. This issue is, of course, of concern for missiles at all speeds, but is particularly important as the speed increases. The optimisation of normal force or side force leads naturally to the evaluation of non-axisymmetric bodies to assist in generating greater normal (or side) forces.

This paper concentrates on the problem areas of kinetic heating and ablation alleviation, particularly at stagnation points, kinetic heating and incipient separation on seeker windows, with reference to multispectral seeker geometries, and interference heating due to aerodynamic controls (fins and reaction jets). We assume, for the purposes of this paper, that the gas is thermally and calorically perfect. The general conclusions made here are relevant also to high temperature gas effects. The emphasis is on the physical attributes and difficulties of prediction for such complex flowfields.

## 2 Interference Heating

Only for the simplest of axisymmetric hypersonic missile shapes, such as cones and cone cylinders at zero angle of attack, do relatively simple methods exist for the prediction of aerodynamic heating (see for example Anderson [1]). The addition of stabilising devices such as fins and flares, the use of aerodynamic surfaces for generating lateral accelerations, the use of control jets and departures from axial symmetry, all introduce significant departures from these simple predictions. Features of many of the resulting flow fields are flow separations and reattachments. These make heat transfer predictions difficult, particularly when the boundary layer state is transitional or turbulent, yet it is in such flow regions where there can be very large increases in heat transfer compared with the interference free flow condition. It is the purpose of the following sections to highlight the physical aspects of some examples of hypersonic flow interference effects on heat transfer. The discussion is based on a survey of some experimental results, principally obtained at the University of Southampton, for a) ramp flows on flat plates (simulating a flared body), b) unswept and swept fins on a flat plate and c) axisymmetric control jets issuing perpendicular to a flat plate. Many of the heating measurements have been made using the liquid crystal thermography technique, as described in the review by Roberts and East [2]. Whilst these results are not directly applicable

to the more complex flows arising from fins, flares or jets on the more usual axisymmetric missile body shapes, the physical properties highlighted in these studies do provide insight into the broad features expected on more realistic geometries and indicate some of the problem areas for future study.

### 2.1 Interference heating on deflected flaps or flares

The essential flow features of the shock-boundary layer interaction arising from a deflected flap or a flared after-body on a missile shape are shown schematically in Fig 1.

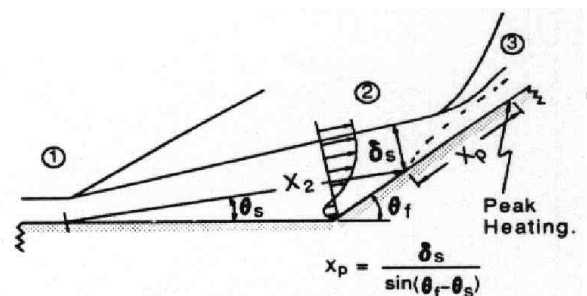


Fig 1. Schematic of the compression corner separated flow; after Smith [5].

Above a certain deflection angle, which is a function of the free stream Mach number and the Reynolds number at the flap/plate junction, the flap shock is of sufficient strength to promote incipient separation. Needham and Stollery [3] have explored the conditions for hypersonic laminar incipient separation. A simple correlation criterion for the flap angle  $\theta_{is}$  (in degrees) for incipient separation at a free stream Mach number  $M_\infty$  at the edge of the oncoming boundary layer is

$$M_\infty \theta_{is} = k\chi^{1/2}$$

where  $\chi$  is the viscous interaction parameter,  $M_\infty^3 Re_L^{-1/2}$ , and  $k$  is a constant in the range 70 - 80 depending on the ratio of the surface temperature to the adiabatic wall temperature. For flap angles above the incipient separation condition, the oncoming boundary layer separates from the plate and the separated shear layer thins considerably in reattaching on the surface of the flap/flare. This results in intense

heat transfer in the reattachment zone. For boundary layers that were laminar before separation, the heating can be exacerbated by transition in the free shear layer before reattachment. For turbulent boundary layers the broad features of the flow field are retained, but incipient separation angles are higher and separation lengths are considerably shorter. For more information on turbulent hypersonic shock boundary layer interactions, involving flat plates and other shapes more appropriate to missile geometries, the reader is referred to an extensive data base compiled by Settles and Dodson [4].

The region of highest aerodynamic heating is a short distance downstream of the reattachment line in the zone where the reattached shear layer thins and a new boundary layer is formed on the flap. Correlations of the peak heat transfer coefficient  $h$ , defined as  $q_w/(T_{aw} - T_w)$ , are shown in Figs 2.

In Smith's [5] experiments, in which the flow fields were laminar at separation, but transitional/turbulent at reattachment, peak heat transfer coefficients of up to 60 times the undisturbed flat plate values were measured. In Fig 2 the characteristic correlations for fully laminar and fully turbulent interactions are shown. This figure also demonstrates that the peak heating for transitional flows may be in excess of the fully turbulent correlations.

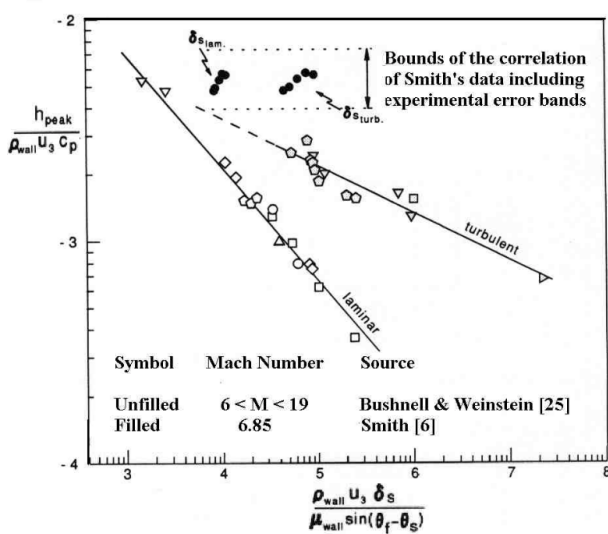


Fig 2. Bushnell & Weinstein [25] correlation of peak reattachment heating for laminar and turbulent wedge separated flows; after Smith [5].

The variation of the heat transfer rate, as described by the Stanton number, throughout the separation zone and at and downstream of reattachment is illustrated in Fig 3. These measurements, obtained by Smith [5] using thin film heat transfer gauges, are correlated in this figure with schlieren and liquid crystal surface thermography measurements. They emphasise the intense reattachment heating following downstream of the separated flow region in which the heating rate is initially reduced before the effect of transition in the free shear layer causes it to increase before the flap/plate junction is reached. A further feature evident from the surface thermograph shown in Fig 3 is the distribution of streamwise striations downstream of reattachment. These are classical Görtler [6] type vortices resulting from instability due to flow curvature just

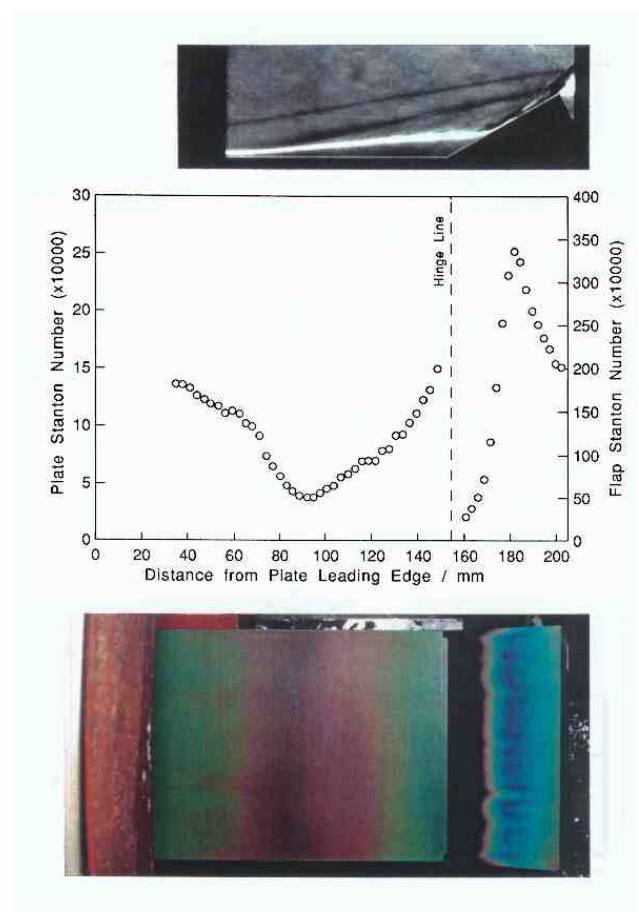


Fig 3. Comparison of schlieren flow visualisation, thin film gauge measurements and liquid crystal thermography. Flap angle = 30°,  $M_\infty = 6.85$ ,  $Re_\infty = 2.45 \times 10^6/m$ ; after Smith [5].



downstream of reattachment. Many observations of these streamwise vortices have been made downstream of laminar reattachments (for example, Henckels et al [7], but Smith and East [8] have also observed these features for transitional and turbulent reattachments. A result of these three-dimensional features of the flow downstream of reattachment is the lateral non-uniformity of the heat transfer in this region.

The incipient separation of turbulent boundary layers is more complex than the above arguments suggest. Babinsky and Edwards [9] observed that at a cylinder-flare junction at Mach 5, separation, as determined from the use of high resolution liquid crystal thermography, appeared to occur at lower flare angles than would be expected based on the existing criteria. Figure 4 shows flow visualisation at a cylinder-flare junction with flare angles of 15 and 20°. They estimated that the height of the separation bubble that they were observing was of the order of 3% of the boundary layer thickness with increases in heat transfer of up to factors of three for a 20° flare. This is significant in missile design, for example, at material interfaces. The small size of the bubble led Babinsky and Edwards to conjecture that this was essentially a laminar phenomenon. Furthermore, since the bubble was small in terms of boundary layer thickness, the perturbation to the external flow was negligible for flare angles less than about 20°.

It is intriguing to note that Edwards and Roper [10] computed the experimental flows with a Baldwin-Lomax turbulence model and obtained good qualitative agreement for the pressure and separation structure. The Baldwin-Lomax model, of course, does not model the laminar sublayer explicitly. For the boundary layer that they grew, it was shown that the separation bubble increased in size with increase in flare angle to accommodate a constant maximum pressure gradient at which separation occurred.

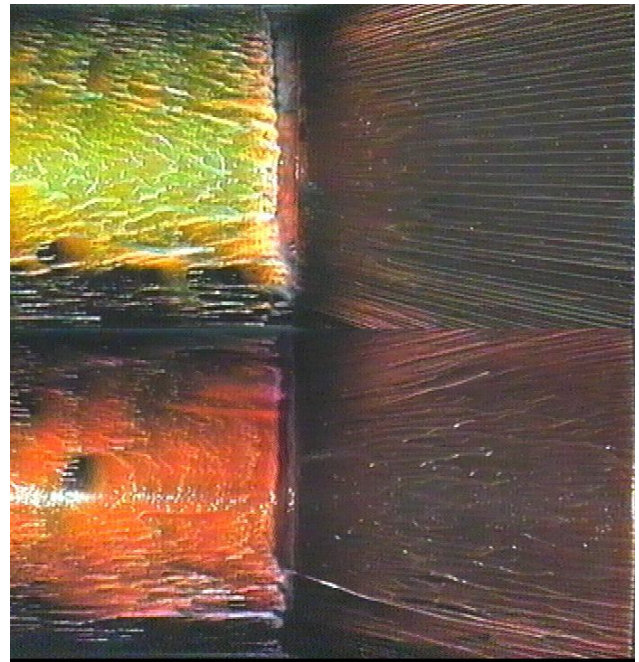


**Fig 4. Flow visualisation of cylinder flare junction showing boundary layer separation at Mach 5. 15° flare (lower) and 20° flare (upper). After Babinsky and Edwards[9].**

### 3 Fin Induced Interactions

#### 3.1 Sharp fin induced interactions

The shock waves generated by aerodynamic surfaces used to generate lateral accelerations and/or provide directional stability and control, interact with the main body boundary layer, causing complex flow fields featuring flow separations and reattachments that can lead to intense local heating. The magnitude of these effects is a function of the sweep and bluntness of the surface and the state of the body boundary layer. Fully laminar interactions often result in steady flows, but for oncoming turbulent boundary layers the interaction is inherently unsteady and may result in significant fluctuating aerodynamic loads in the interaction region.

A schematic of the flow field resulting from a single sharp fin/turbulent boundary layer interaction at  $M = 6.2$  as proposed by Haq [11] is shown in Fig 5. At fin incidence angles near zero the fin shock is too weak to promote lateral separation, but a small region of separated flow is noted at the apex of the fin and a corner

vortex results at the fin/plate junction. As fin incidence increases, the fin shock separates the plate boundary layer and the primary vortex shown in Fig 5 results. For even greater fin incidences the existence of a pocket of secondary separated flow beneath the primary vortex has been observed [11].

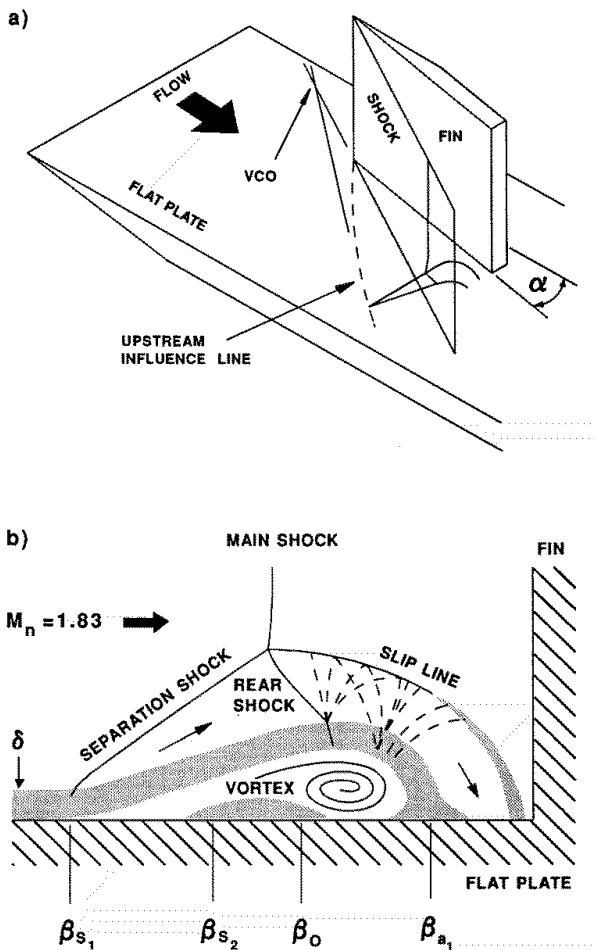


Fig 5. Proposed flow structure for the sharp unswept fin interaction; after Haq [11].

Heat transfer contours on the plate surface obtained from liquid crystal thermography are shown in Fig 6. These demonstrate the quasi-conical nature of the flow, but with an origin slightly ahead of the fin leading edge. The contours also show the embedded secondary separation and the high heat transfer rate in the reattachment between the primary and corner vortices. The magnitude of the heat transfer enhancement above the undisturbed value on plate is shown in Fig 7. In this figure, distributions perpendicular to the fin surface are compared for the cases of swept and unswept

fins at 20° incidence at various positions downstream of the fin leading edge. These clearly show the existence of the embedded vortex and the magnitude of the peak heat transfer at reattachment close to the fin/plate junction. It should be noted that the magnitude of the peak heat transfer is probably underestimated, due to the limited range of sensitivity of the liquid crystals used for the measurements.

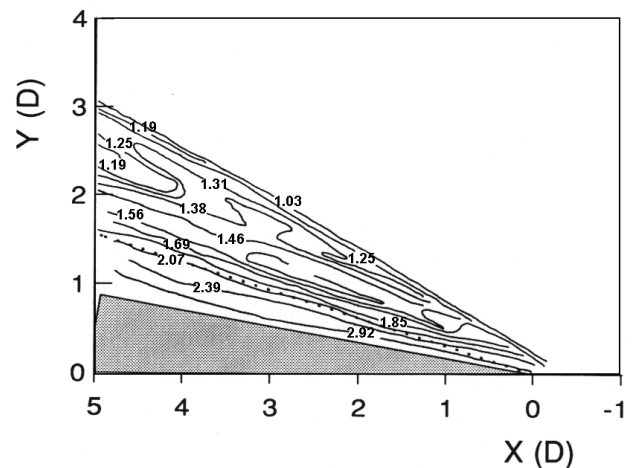


Fig 6. Normalised heat transfer ( $h/h_u$ ) contours around a sharp unswept fin inclined at 15° incidence.  $M_\infty = 6.2$ ,  $Re_\infty = 40 \times 10^6/m$ ,  $\delta_{fin} = 4.5 \text{ mm}$ ; after Haq [11].

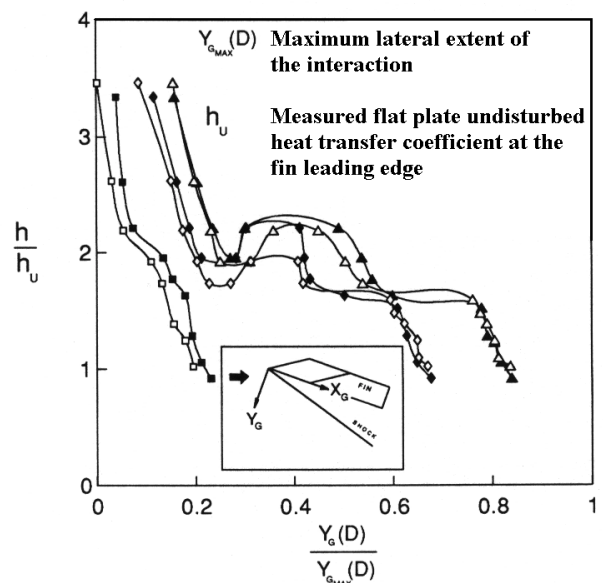


Fig 7. Comparison of normalised lateral heat transfer profiles at different downstream stations for 25° swept ( $x_G=0.5D$ ,  $\phi x_G=3D$ ,  $\Delta x_G=4D$ ) and unswept fins ( $v x_G=0.5D$ ,  $v x_G=3D$ ,  $\sigma x_G=4D$ ) at 20° incidence at  $M_\infty = 6.2$ ,  $Re_\infty = 40 \times 10^6/m$ ; after Haq [11].

### 3.2 Blunt fin induced interactions

In practice, the leading edge of fin stabilisers may be blunted, either to alleviate stagnation line heating, or as a result of ablation as the missile proceeds along its trajectory. However, the strong bow shock resulting from leading edge bluntness causes a much more extensive and stronger interaction with the body boundary layer than in the case of the sharp leading edge described in section 3.1. These problems have been extensively studied experimentally, but the resulting flow fields are of considerable complexity and represent formidable computational challenges, particularly in the case of turbulent boundary layer interactions for which appropriate turbulence models are lacking in the regions of the flow that are subject to the intense interaction. In order to bring out the physical features of these flows some experimental results obtained at the University of Southampton for laminar interactions by Schuricht [12] and for turbulent interactions by Haq [11] will be described.

Schuricht [12] studied blunt fin/laminar boundary layer interactions on a flat plate at  $M = 6.7$  and Reynolds number of  $7.6 \times 10^6/m$  and investigated the effects of fin leading edge diameter, sweep and angle of incidence. Liquid crystal thermography and surface oil flow techniques were used to obtain physical insight and quantitative heat transfer measurements were made. The broad features of the interaction are illustrated in Fig 8. This compares the oil flow and liquid crystal response for an unswept blunt fin at zero incidence. The upstream influence of the bow shock/laminar boundary layer interaction extends some 4 diameters upstream of the leading edge and the lateral extent of the interaction reaches more than 6 diameters at a position 2 diameters downstream of the leading edge. The principal features of the flow field are the numerous horseshoe vortices wrapped around the leading edge and the resulting separations and reattachments characterised by reduced and enhanced heating levels. The levels of the peaks and troughs in heat transfer diminish with distance from the fin and the region of most intense heating on the plate surface close to the fin leading edge,

which was in excess of 10 times the undisturbed value, caused the liquid crystal layer to ablate. In these particular experiments four primary and four secondary vortices were observed from surface flow features. When the highly three-dimensional nature of the whole flow field is noted, the complexity of the computational modelling required to predict such flows is apparent.

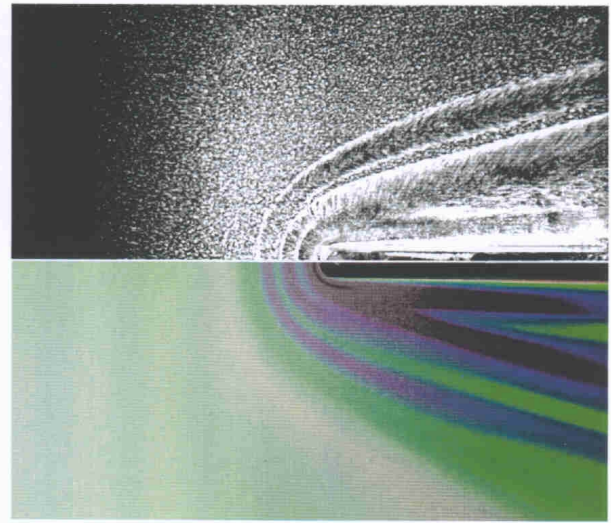


**Fig 8. Oilflow (upper) and liquid crystal response (lower) for an unswept blunt fin of leading edge diameter 5 mm in laminar hypersonic flow at  $M_\infty = 6.7$ ,  $Re_\infty = 7.6 \times 10^6/m$ ; after Schuricht [12].**

For unswept blunt fins, the extent of the interaction broadly scales with fin diameter and the levels of heat transfer do not appear to be affected greatly. This is demonstrated in Fig 9, which gives a good correlation for the interaction geometry, but some variations in the heat transfer levels near the fin leading edge are observed. The peak values of six times the undisturbed values are an underestimate of the true magnitude due to the erosion of the liquid crystals in this region.

For swept blunt fins Schuricht [12] has shown that both the extent of the interaction and the peak heating levels are significantly reduced. These effects are summarised in Fig 10, which shows that the peak heating values are reduced from in excess of 10 times the undisturbed value for unswept blunt fins to less



than 2 times for 60° sweep. Furthermore, the complexity of the interaction reduces with sweep; fewer vortices and hence regions of separation and reattachment are observed.

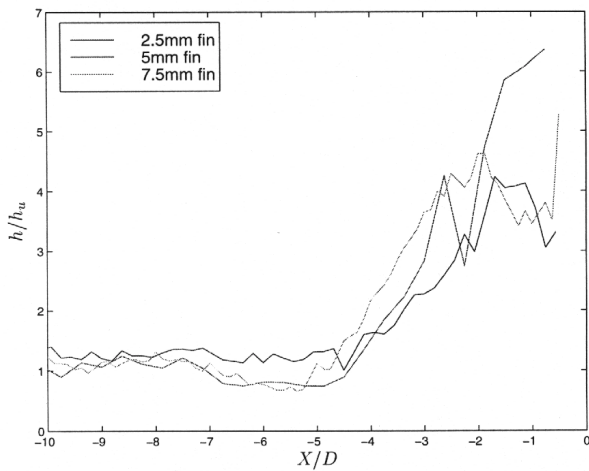


**Fig 9. Comparison of centreline normalised heat transfer coefficients for different fin diameters at  $M_\infty = 6.7, Re_\infty = 7.6 \times 10^6/m$ ; after Schuricht [12].**

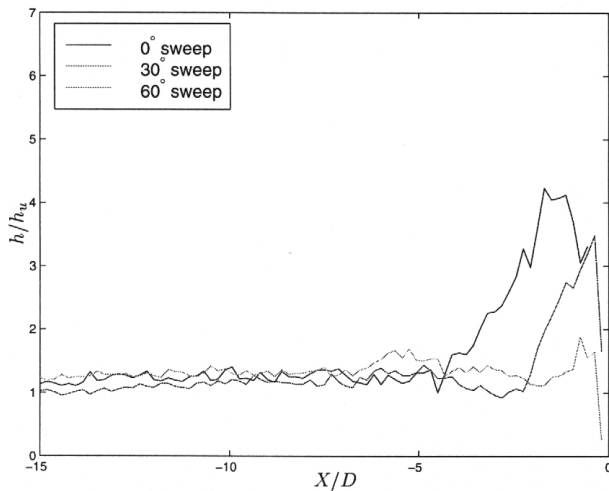


**Fig 10. Comparison of centreline heating for varying angles of sweep ahead of blunt fins at  $M_\infty = 6.7, Re_\infty = 7.6 \times 10^6/m$ ; after Schuricht [12].**

The effect of increase in the fin incidence is characterised by a region close to the fin leading edge where the flow structure is essentially unaltered from the zero incidence case, but further downstream the flow field bears more similarity to the conical character associated with sharp fin flow structures.

However, overall heat transfer levels appear to increase slightly with incidence.

For the case of turbulent boundary layers upstream of the fin, Haq [11] studied a similar range of parameters to those described above. In comparison with the laminar interaction, the extent of the upstream influence ahead of the leading edge is less (between 2 and 3 diameters upstream), as is also the lateral influence (between 5 and 6 diameters at 2 diameters downstream from the leading edge). Surface heat transfer contours obtained by Haq using liquid crystal thermography are shown in Fig 11.

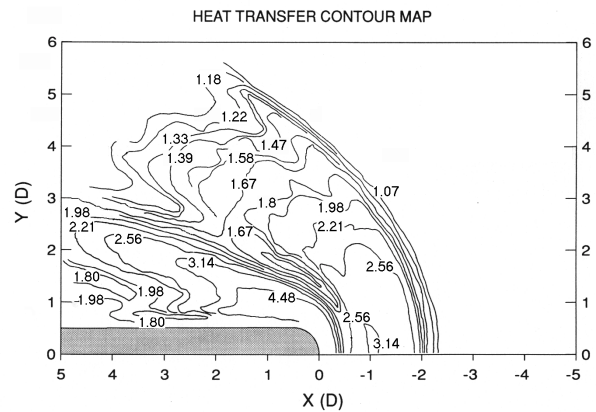


**Fig 11. Normalised heat transfer ( $h/h_u$ ) contours around a blunt unswept fin at zero incidence.  $M_\infty = 6.2, Re_\infty = 40 \times 10^6/m, D = 10 \text{ mm}, \delta_{in} = 4.5 \text{ mm}$ ; ( $h_u$  is the undisturbed heat transfer coefficient at the fin leading edge); after Haq [11].**

This shows the complexity of the flow structure that is dominated by the characteristic horseshoe vortices as for the laminar interaction. The flow fields were broadly similar to those found by other workers, for example Stollery *et al* [13], at different supersonic Mach numbers. Haq proposed a flow model that consisted of primary and secondary separations along the fin centre line ahead of the leading edge, together with embedded tertiary separation that leads to the formation of a multiple horseshoe vortex necklace within the interaction region.

Haq studied the effects of only two leading edge diameters, but the broad features of the heating pattern appeared to scale with fin leading edge diameter. Similar to the results for the laminar interaction, the flow fields were

approximately independent of incidence in the nose region and became more conical in character further downstream as incidence was increased. As shown in Fig 12, the peak heating values were in excess of 7 times the undisturbed values close to the fin leading edge, but the precise location and magnitude of the peak heating could not be measured due to erosion of the liquid crystal coating.

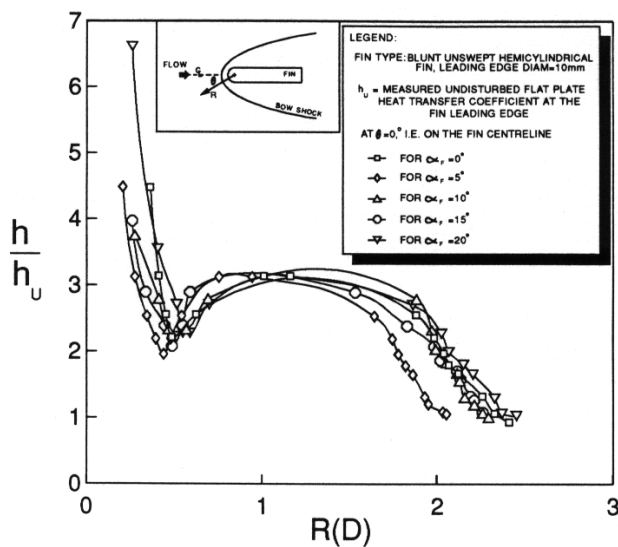
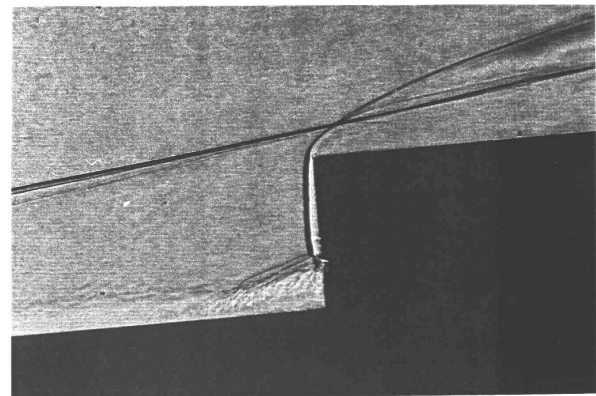


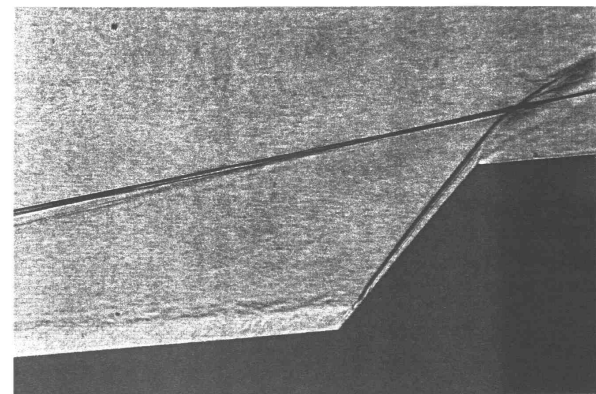
**Fig 12. Comparison of the centreline heat transfer profiles ahead of a blunt unswept fin at  $0^\circ$  ( ),  $5^\circ$  (◇),  $10^\circ$  (△),  $15^\circ$  (○) and  $20^\circ$  (▽) inclinations at  $M_\infty = 6.2$ ,  $Re_\infty = 40 \times 10^6/m$ ,  $D = 10$  mm,  $\delta_{fin} = 4.5$  mm, ( $h_u$  is the undisturbed heat transfer coefficient at the fin leading edge); after Haq [11].**

A further feature of the interaction is the intense heating experienced on the fin leading edge due to a supersonic jet impinging on the surface downstream of the region where the separation shock interacts with the fin bow shock leading to an Edney type IV interaction [14]. This is illustrated in the schlieren photograph shown in Fig 13a. Fig 13b shows a comparable photograph for a  $45^\circ$  swept blunt fin in which the separation ahead of the fin is suppressed and there is no evidence of the Edney type IV interaction. This phenomenon has also been observed in the free-flight experiments of Dupuis and Edwards [15] for the case of a cone/cylinder/flare model with 8 rectangular unswept fins with bevelled leading edges. In these experiments considerable

ablation of the fin leading edges occurred and the peak erosion was measured in the region where the Edney type interaction would be expected. At the same time, catastrophic fin failure occurs close to the expected position of the attachment line of the primary horseshoe vortex (see Figs 4 and 7) along the side of the fin [16].



(a)



(b)

**Fig 13. Schlieren photographs of the shock structure ahead of blunt fins at  $M_\infty = 6.7$ ,  $Re_\infty = 40 \times 10^6/m$ ,  $D = 10$  mm,  $\delta_{fin} = 4.5$  mm; a) unswept, b)  $45^\circ$  sweep; after Haq [12].**

Sweeping the fin leading edge also has the merit of reducing the attachment line heating, since this depends on the normal Mach number of the approaching flow [1]. However, Poll [17] has demonstrated that as the sweep increases, and with it, as the cross flow Reynolds number increases, the flow at the attachment line can



become turbulent. The situation is exacerbated by contamination from the body boundary layer, so essentially the cross flow Reynolds number needs to be sufficiently low that the flow relaminarises. Since heat transfer from a turbulent boundary layer is of the order of three times that from a laminar boundary layer, as sweep increases the heat transfer can actually rise.

It is important to note that all of Haq's measurements are from time averaged measuring techniques. However it is well established that the interactions involving turbulent boundary layers are inherently unsteady in nature. Dolling [18] (for example), has made extensive investigations using time resolved techniques for flap, fin and glancing shock induced separations and has demonstrated the importance of correctly modeling these unsteady phenomena in predicting the properties of these flow fields. This work emphasises the importance of correctly modeling the turbulence structure for these complex flows, particularly in the context of predicting the heat transfer rates. Tutty et al [19] compared the results of Haq for the blunt unswept fin interaction with predictions using a Navier-Stokes code using a Baldwin-Lomax turbulence model. Although good predictions were obtained for the general shape of the interaction zone, some discrepancies were noted in the scale of the interaction. The centre line heating distribution was in reasonable agreement with measurements, although the peak heating was locally predicted to be some 25 times the undisturbed value at the base of the fin body junction due to the small corner vortex. At the same time, the correct prediction of the whole flowfield is a significant problem, for the general case, due to the growth of a new laminar boundary layer at the fin stagnation line, outboard of the interaction region. Due to the thickness of the boundary layer, very small cells are required which increases the computational time dramatically.

The discussion of fin and interference heating above, demonstrates the importance and magnitude of the effects. Moreover, the problem in limiting heat transfer to ensure the survival of

fins or empennages employed as aerodynamic control surfaces may be insuperable for small vehicles flying at high Mach number in the lower atmosphere for significant duration. As an alternative to aerodynamic control surfaces, reaction control jets may prove attractive for certain missions.

### **3.3 Transverse jet induced interactions**

It has been well established that transverse jets are possible means of control of hypersonic missiles. For two-dimensional slot jets Powrie [20] has shown that as a result of the interaction with the wall boundary layer, the side force generated is amplified over the pure jet thrust by factors in excess of 4 for slot jets at  $M = 6.7$ . For the more practical case of axisymmetric jets, the amplification factors are lower and Powrie [20] measured values of up to 3 for sonic jets issuing normal to a flat plate at  $M = 6.7$ . The interactions on axisymmetric bodies are more complex and amplification factors are dependent on body shape and the presence of aerodynamic surfaces. For example, Brandeis and Gill [21] measured values between 1 and 1.6 as the angle of attack varied from zero to  $10^\circ$  for an ogive cylinder with a normal circular jet at  $M = 8$  and higher values up to 2.2 were obtained by tilting the jet forward by  $30^\circ$ . In contrast, the same authors [22] found that the addition of aerodynamic surfaces of various geometry to the same basic shape increased the amplification factor at near zero angles of attack, but only small amplification factors were obtained at small angles of attack.

With regard to heat transfer, it can be argued that there is some similarity between the interaction resulting from a transverse jet and that caused by a circular cylinder, or a blunt fin leading edge perpendicular to the flow. It is evident, therefore, that the potential for significant interference heating exists from the use of transverse control jets. Examples taken from recent work at the University of Southampton will be used to illustrate these effects.

The principal features of the three-dimensional development of the flow field resulting from the interaction from a circular jet

are shown schematically in Fig 14. This demonstrates the broad similarity with the flow field around a blunt fin, with the existence of possibly several horseshoe vortices. A principal feature of the jet interaction flow field is the entrainment of the high enthalpy free stream fluid and its subsequent effect on the primary reattachment zone downstream of the interaction. This is potentially a region of very intense heat transfer.

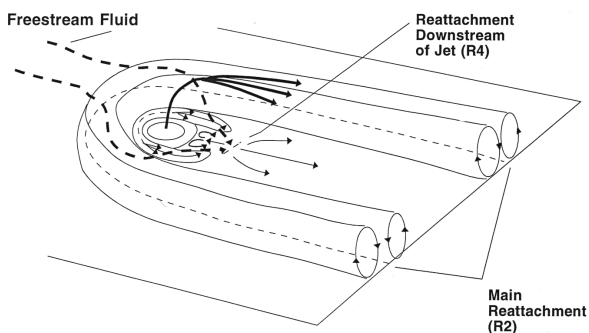


**Fig 14. Interpretation of the flow field downstream of an axisymmetric jet; after Powrie [20].**

Powrie [20] extensively studied the flow fields, pressure distributions and forces arising from the interaction of sonic jets of different composition issuing normal to a laminar hypersonic boundary layer at  $M = 6.7$ . In contrast with the results for two-dimensional jets, it was found that the specific heat ratio and molecular weight of the jet gas had significant effects on the flow fields and the force coefficients. This was attributed to the variations in the jet plume width with gas composition. Although Powrie did not obtain any quantitative heat transfer measurements, it was demonstrated through the qualitative use of liquid crystals that large increases in heat transfer existed in the primary reattachment region downstream of the jet.

This phenomenon was subsequently investigated in more detail by Mudford et al [23] and by Schuricht [12] using quantitative liquid crystal thermography. In these experiments Ar, He, N<sub>2</sub> and CH<sub>4</sub> at 20°C were injected through a choked circular orifice into a nitrogen free stream ( $M = 6.7$  and Reynolds

number of  $4.3 \times 10^6/m$ ). Heat transfer distributions were obtained on the plate surface, an example of which is shown in Fig 15 for the case of argon injectant. This demonstrates the peaks and troughs in the heat transfer rate in the region upstream of the jet associated with the reattachments and separations described previously. It also shows that the highest peaks in heat transfer exist downstream of the interaction in the primary reattachment zone. The values of the ratios of the peak heat transfer to the undisturbed values were found to be highest for argon injectant (5.34 for injectant pressure  $p_j = 1\text{bar}$ ) compared with 3.22 for helium, 3.73 for nitrogen and 2.64 for methane at the same injectant pressure. Increase of injectant pressure resulted in higher peak values (7.25 for argon at  $p_j = 1.6\text{ bar}$ ) and there was evidence that the peaks were still increasing at the downstream limit of the plate used in the investigation.

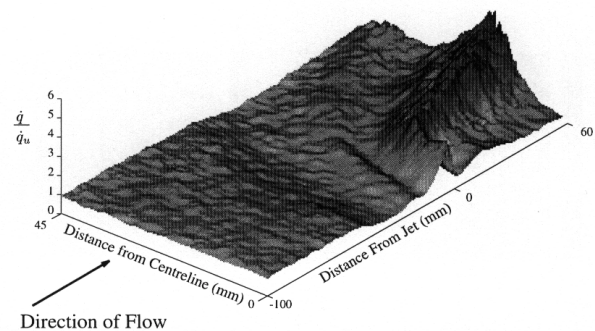


**Fig 15. Isometric plot of the normalised heat transfer distribution around a normal argon jet ( $p_j = 1\text{ bar}$ ) into nitrogen at  $M_\infty = 6.7$ ,  $Re_\infty = 7.6 \times 10^6/m$ ; after Mudford et al [23].**

The details of the interacting flow fields are clearly complex, involving massive separations, multiple embedded vortices and mixing between the free stream and the injectant gases. Recently, Qin and Redlich [24] have used a laminar Navier-Stokes code to provide comparisons with the experimental results of Powrie [20] for the injection of a two-dimensional sonic jet. Good agreement was obtained for the flow field geometry and pressure distributions, but no heat transfer predictions were made. Extension of the modeling to the axisymmetric case, to include

the effect of heat transfer is needed. The effect of the interaction on transition of the separated shear layer is also a problem of some importance in determining whether the primary reattachment region in which the peak heating occurs is transitional/turbulent even when the separation is laminar. Furthermore, as in the case of ramp and fin induced separations of turbulent boundary layers, the jet induced interaction is likely to be inherently unsteady in nature. All of these features introduce significant complications to modeling the jet interaction problem for more realistic missile shapes and flow conditions and present formidable computational challenges.

#### 4 Concluding Remarks

For the simple geometries of the flow over a compression corner, at a deflected flap or flare, for example, the question of incipient separation was discussed. The point at which the boundary layer is seen to detach and then reattach is shown to be important from the point of estimation of the large heat transfer rate at attachment points. For laminar boundary layers there are simple criteria, but for turbulent boundary layers, while there are correlations, there is some doubt in the validity of these when looking at the boundary layer with high spatial resolution. This is an important issue, since while for laminar boundary layers the heat transfer rate at reattachment can be 60 times the undisturbed value, an increase in heat transfer rate of 2 or 3 may be of significance at seeker window facets. It is also noted, that while the geometries are nominally two-dimensional the possible development of Görtler vortices generates three-dimensional effects.

For sharp fin induced interactions it was shown that the heat transfer distribution on the body appears to be conical with the heat transfer rate peaking at attachment of the flow close to the fin-plate junction. As the fin angle increases, the flow separates, and the total thermal loading increases substantially.

For blunt fins, it is shown that the aerodynamic interference is more complex than for sharp fins. Unswept blunt fins invariably

separate the flow leading to Edney type IV interactions with dramatic effects on heat transfer to the fin. In addition, it is noted that the vortical structures associated with blunt fin interactions are very complex. For swept blunt fins, the extent of separation can be limited, due to the weaker bow shock. However, heat transfer to the body is still significant. Remarks were also made regarding reductions in heat transfer rate to the fin leading edge by increasing fin sweep, but with the possible danger of attachment line contamination as sweep increases.

Reaction control jets can offer significant advantages over deployed aerodynamic surfaces for sustained hypersonic flight since the associated heating is present only when undertaking manoeuvres. Nevertheless, prediction of the heat transfer rates is still required. It is noted that the nature of the flowfield is still complex, and has broad similarity with the flow about a blunt fin. Heat transfer rates were observed to be dependent on the injected (cold) gas and on the stagnation pressure of the injectant. In the experimental data discussed here, heat transfer rates reached levels of over seven times the undisturbed value. Another major issue in the use of such jets is the prediction of the amplification factors. This is dependent on geometry and requires accurate prediction of the three-dimensional separated flowfield.

This paper has outlined some of the kinetic heating problem areas involved in the design and analysis of hypersonic missiles. Here we have concentrated predominantly on aspects of interference heating where our understanding of the physics is limited. These issues tend to involve highly non-linear aerodynamics and are difficult to predict, even with current high speed computers. There are two major issues concerning the computational prediction of such complex high speed flows. Firstly, the geometries are three-dimensional and involve significantly different spatial scales, leading to meshing problems and the solution of the Navier-Stokes equations on large meshes. Secondly, there is the ever present problem of inadequate turbulence models, made worse by



the experimental difficulties of making high resolution measurements of turbulence quantities in fully developed turbulent boundary layers at hypersonic speed, that we may calibrate such models. If we also consider the effects of high temperature, reacting gases, or rarefied gases, the problems are compounded many times.

## References

- [1] Anderson J D Jr. Hypersonic and High Temperature Gas dynamics. McGraw-Hill. (1989).
- [2] Roberts G T and East R A. Liquid crystal thermography for heat transfer measurement in hypersonic flows: a review. *Journal of Spacecraft and Rockets*, Vol.33, No.6, pp 761-768, 1996..
- [3] Needham D A and Stollery J L. Hypersonic studies of incipient separation and separated flows. AGARD Conf. Proc. No. 4, Separated Flows, Part 1, 1966.
- [4] Settles G S and Dodson L J. Supersonic and hypersonic shock/boundary layer interaction database. *AIAA Journal*, Vol.32, No7, pp 1377-1383, 1994.
- [5] Smith A J D. The dynamic response of a wedge separated hypersonic flow and its effects on heat transfer. University of Southampton PhD Thesis, 1993.
- [6] Görtler H. Über ein dreidimensionale instabilität laminarer grenzschichten an konkaven wänden. *Nachr. Ges. Wiss., Göttingen, Math. Phys. Kl. 1*, p1; see also NACA TM 1375, 1949.
- [7] Henckels A, Kreins A F and Maurer F. Applications of infrared measurement technique in hypersonic facilities. In *Shock Waves* (ed. Takayama K) Vol. 1, pp 651-656, 1992.
- [8] Smith A J D and East R A. Unpublished work, 1992.
- [9] Babinsky H and Edwards J A. On the incipient separation of a turbulent hypersonic boundary layer. *The Aeronautical Journal*, Vol.100, pp 209-214, 1996.
- [10] Edwards J A and Roper J J. Computational investigation of the incipient separation of a hypersonic turbulent boundary layer. *AIAA Paper 97-0769*, 1997.
- [11] Haq Z U. Hypersonic vehicle interference heating. University of Southampton PhD Thesis, 1993.
- [12] Schuricht P H. Liquid crystal thermography in high speed flows. University of Southampton PhD Thesis, 1999.
- [13] Stollery J L, Fominson N R and Hussain S. The effects of sweep and bluntness on glancing interactions at supersonic speeds. *ICAS Paper No. 86-1.2.1*, 1986.
- [14] Edney B. Anomalous heat transfer and pressure distributions on blunt bodies at hypersonic speeds in the presence of an impinging shock. FFA (Aeronautical Research Institute of Sweden) Report 115, 1968.
- [15] Dupuis A D and Edwards J A. Free-flight tests, analysis and aeroheating aspects of two hypersonic configurations. 15<sup>th</sup> International Symposium on Ballistics, Jerusalem, 1995.
- [16] Edwards J A and Dupuis J A. Free -flight tests of fin heating and ablation at Mach 5 and 6. *AIAA Paper 00-0555*, 2000.
- [17] Poll D I A. The effect of wing sweep back upon transition in hypersonic flow. *AIAA Paper 95-6090*, 1995.
- [18] Dolling D S. High speed turbulent separated flows: consistency of mathematical models and flow physics. *AIAA Journal*, Vol.36, No.5, pp 725-732, 1998.
- [19] Tutty O R, Roberts G T, East R A, and Huntington-Thresher W. Numerical study of fin-body interference effects at hypersonic speeds. In *Proceedings of the Second European Symposium on Aerothermodynamics for Space Vehicles*, ESTEC, pp 51-56, 1995.
- [20] Powrie H E G. A study of the interaction between an underexpanded normal jet and a hypersonic free stream. University of Southampton PhD Thesis, 1996.
- [21] Brandeis J and Gill J. Experimental investigation of super- and hypersonic jet interaction on missile configurations. *Journal of Spacecraft and Rockets*, Vol.35, No.3, pp 296-302, 1998.
- [22] Brandeis J and Gill J. Experimental investigation of side-jet steering for supersonic and hypersonic missiles. *Journal of Spacecraft and Rockets*, Vol.33, No.3, pp 346-352, 1996.
- [23] Mudford N R, Roberts G T, Schuricht P H, Ball G J and East R A. Interference heating caused by a 3D transverse jet in hypersonic flow. In *Shock Waves* (eds. Sturtevant B, Shepherd J E and Hornung H G) Vol. 1, pp 173-178, 1995.
- [24] Qin N and Redlich A. Massively separated flows due to transverse sonic jet in laminar hypersonic stream. *Shock Waves*, Vol.9, pp 87-93, 1999.
- [25] Bushnell D M and Weinstein L M. Correlation of peak heating for reattachment of separated flows. *Journal of Spacecraft*, Vol.5, No.9, pp 1111-1112, 1968.